

Universal magnetic oscillations of conductivity in the incoherent regime of correlated systems

Jakša Vučičević¹ and Rok Žitko^{2,3}

¹Scientific Computing Laboratory, Center for the Study of Complex Systems, Institute of Physics Belgrade, University of Belgrade, Pregrevica 118, 11080 Belgrade, Serbia

²Jožef Stefan Institute, Jamova 39, SI-1000 Ljubljana, Slovenia

³Faculty of Mathematics and Physics, University of Ljubljana, Jadranska 19, SI-1000 Ljubljana, Slovenia

(Dated: April 30, 2022)

We investigate the magnetic field dependence of conductivity in the Hubbard model on the square lattice. Fully taking into account the orbital effects of the field introduced via the Peierls substitution, we perform extensive computations using the dynamical mean-field theory. In addition to the conventional Shubnikov-de Haas quantum magnetic oscillations, associated with the coherent cyclotron motion of quasiparticles and the presence of a well-defined Fermi surface, we find an additional oscillatory component with a higher frequency that corresponds to the total area of the Brillouin zone. This paradigm-breaking magnetic oscillation appears due to the incoherent excitations at elevated temperatures. It is a purely transport effect and has no counterpart in the thermodynamic or spectral properties of the system. Its origin can be traced back to the structure of the current vertex in the presence of the magnetic field, hence it is a kinematic rather than a dynamic effect.

The strong effect of the Lorentz force on the motion of charge carriers in metals manifests as quantum oscillations (QOs) [1]. All system properties – thermodynamic (magnetisation, chemical potential), dynamic (scattering time), and transport (resistivity, Hall angle) – have periodic components as functions of inverse magnetic field, $1/B$. This is due to the quantized electron orbitals passing through the Fermi surface (FS), hence these effects provide detailed information about the topology of the FS and its shape [1, 2]. The oscillations are observable at low temperatures under the condition of sufficient coherence: $\omega_c\tau > 1$ and $\hbar\omega_c > k_B T$, where $\omega_c = eB/m^*$ is the cyclotron frequency with e the elementary charge, m^* the effective carrier mass, τ the elastic transport scattering time, and T the temperature. In bulk materials the oscillations are easier to observe in magnetisation (de Haas-van Alphen effect) than in transport (Shubnikov-de Haas effect), but the converse is true for thin samples and layered materials [3–5]. In nearly a century that has passed since the discovery of QOs, it was found that they are surprisingly ubiquitous, existing beyond the basic paradigm of simple metals. They were observed in graphite [6, 7], graphene [8, 9], organics [5], cuprates [10–12], perovskite heterostructures [13, 14], iron-pnictide superconductors [15], and most recently in synthetic van der Waals systems, in particular in twisted bilayer graphene [16]. QOs appear in various non-Fermi liquids [17–19] and even in gapped systems such as Kondo insulators [20].

The conventional Lifshitz-Kosevich theory of QOs [2] is a semi-classical single-particle approach. The interaction effects are incorporated through self-energy terms, which are usually assumed to depend only on the quasiparticle energy, but not on its momentum, $\Sigma = \Sigma(\omega)$ [1]. The main effect of moderate interactions is a reduction of the QO amplitude and mass renormalization [1, 21, 22], while strong correlations may lead to more substantial deviations [18]. A very successful method, also within the

approximation of local $\Sigma(\omega)$, but fully applicable in the strong-correlation regime, is the dynamical mean-field theory (DMFT). This approach has been very successful in describing various experiments [23], including transport [24–29]. Recently, it was demonstrated that the orbital effects of the magnetic field can be treated within the single-site DMFT with a translationally invariant impurity problem [30, 31]. We have recently generalized the expression for the dc conductivity [32, 33] within magnetic DMFT theory [34]. State-of-the-art impurity solvers provide access to spectral functions on the real-frequency axis at any temperature [28, 35–38] and for an arbitrary non-interacting density of states, including the one obtained in the presence of strong fields introduced via Peierls substitution [39–41]. The combination of these advances provides a methodology for calculating the Green's functions G as well as the conductivity tensors σ while accounting for the local correlations induced by the electron-electron (e-e) interactions and the effects of the external magnetic field on the orbital motion. The theory comes with no *a priori* restrictions on the temperature, the strength of the e-e interaction, or the external magnetic field. We have applied this to study the Hubbard model on square lattice, obtaining a detailed picture of the SdH oscillations. Unexpectedly, we have also observed an additional oscillatory component with a frequency that corresponds to the *total area of the 2D Brillouin zone* (BZ), which is the topic of the present publication. These highly unconventional QOs become visible with *increasing* temperatures, where they first coexist with the SdH oscillations and even become dominant, before finally being thermally washed out. The frequency is universal in that it does not depend on the Fermi surface properties, but only on the dimensions of the primitive cell of reciprocal space.

Model and method. We consider the Hubbard model on

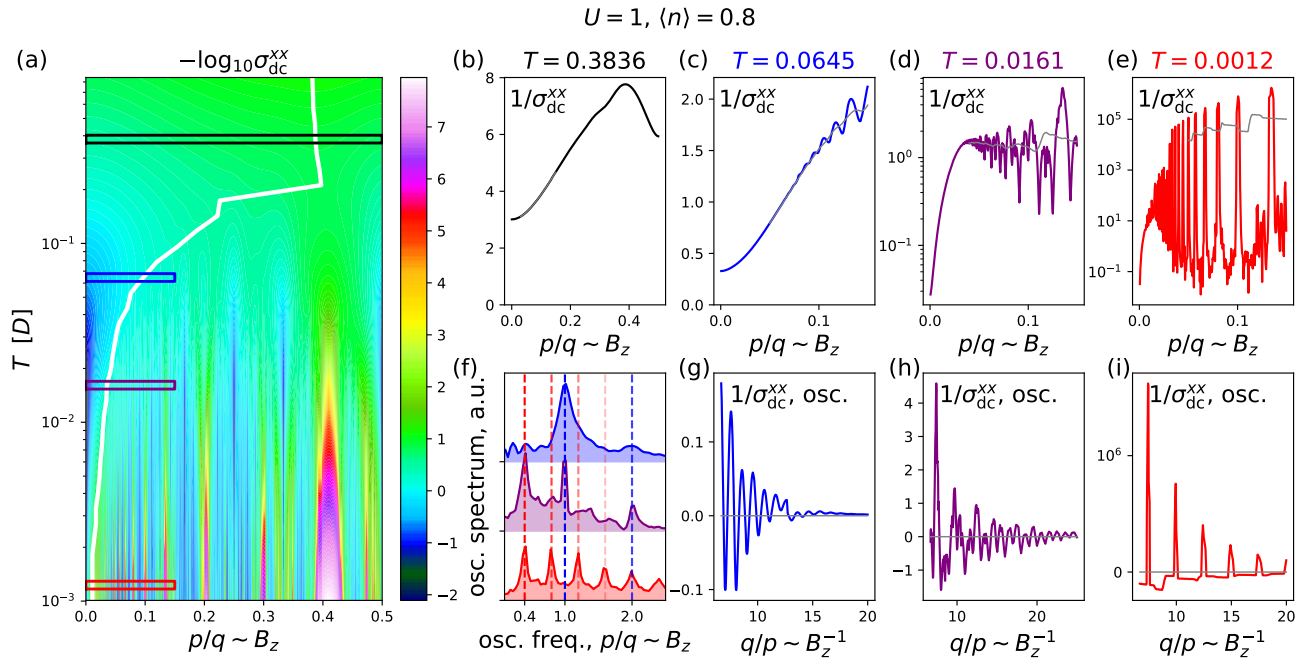


Figure 1. (a) Inverse conductivity $1/\sigma_{dc}^{xx}$ as a function of magnetic field (flux per plaquette p/q) and temperature for the Hubbard model on the square lattice at $U = 1$ and $\langle n \rangle = 0.8$ band filling. Colored rectangles indicate the temperature and the field range of the B dependencies analyzed in the remaining panels. The white line denotes where non-monotonic behavior of $1/\sigma_{dc}^{xx}(B)|_T$ starts. (b,c,d,e) B -dependence of the inverse conductivity. The thin gray line is the background baseline defined as the average over a range of the field of a size proportional to p/q . (f) Frequency spectrum of the QOs obtained as the Fourier transform of the data in panels (g,h,i). Red dashed lines indicate the fundamental frequency and harmonics of the SdH oscillations. Blue dashed lines indicate the HF oscillations. Fourier transforms are performed in the p/q range $0.03 - 0.15$. (g,h,i) Oscillatory component of $1/\sigma_{dc}^{xx}$ versus inverse field, $1/B$, showing SdH oscillations (i, red), HF oscillations (g, blue), or both (h, purple).

a square lattice with the nearest-neighbor hopping

$$H = \sum_{\langle i,j \rangle, \sigma} t_{ij} c_{i\sigma}^\dagger c_{j\sigma} + \sum_i U n_{i\uparrow} n_{i\downarrow}, \quad (1)$$

where i, j enumerate the lattice sites at real-space positions \mathbf{r}_i , $\sigma = \uparrow, \downarrow$, $c_{i\sigma}$ is the electron operator, $t_{ij} = t \exp[i(e/\hbar) \int_{\mathbf{r}_i}^{\mathbf{r}_j} \mathbf{A} \cdot d\mathbf{r}]$ is the hopping integral including the Peierls phase for the vector potential \mathbf{A} , U is the Hubbard e-e repulsion parameter, and $n_{i\sigma} = c_{i\sigma}^\dagger c_{i\sigma}$ is the occupancy-per-spin operator, and we define the site-occupancy as $n = \sum_\sigma n_\sigma$. We use the zero-field half-bandwidth $D = 4t$ as the unit of energy. Given the lattice spacing a , the magnetic flux which passes through a lattice cell is $\phi = Ba^2$; divided by the flux quantum $\phi_0 = h/e$, it yields a dimensionless parameter which we assume to be a rational number, $\phi/\phi_0 = p/q$, in order to obtain a finite magnetic crystall cell [41]. We do not include the Zeeman term [42, 43], as it does not affect the QO frequencies, only their amplitudes, and may be accounted for using a spin reduction factor [1]. The calculation is performed in the absence of disorder and other imperfections, i.e., with the scattering only due to the Hubbard interaction.

In the Landau gauge for the perpendicular magnetic field $\mathbf{B} = B\hat{\mathbf{e}}_z$, the vector potential is given by $\mathbf{A} = Bx\hat{\mathbf{e}}_y$,

and the unit cell dimension is $q \times 1$. Assuming that the self-energy is local, $\Sigma_{ij}(\omega) = \delta_{ij}\Sigma_i(\omega)$, we solve the problem within the DMFT approximation [44–48]. Our theory works best in the limit of sufficiently high temperatures where the locality of Σ is a good approximation [28]. The physical periodicity is not broken in a uniform magnetic field, however the symmetry operation is no longer a pure spatial translation, but rather a magnetic translation operator that includes a Peierls' phase term [49]. Using the gauge invariant Green's function [50], the interacting problem can be reduced to the single-site DMFT self-consistency equation [30, 34]. This is a significant simplification compared to solving q coupled single-impurity problems, one for each site in the magnetic crystall cell [51–54]. At the level of the DMFT, the Kubo bubble can be expressed in a compact form, is gauge invariant and represents the *sole* contribution to the conductivity tensor (there are no vertex corrections). [34] Despite these significant simplifications, the calculation remains computationally demanding and requires an integration over frequencies and a double summation over the non-interacting eigenstates for each wavevector in the reduced BZ. The difficulty is exacerbated by the fact that at small values of p/q a big lattice is required, while at large p/q it is difficult

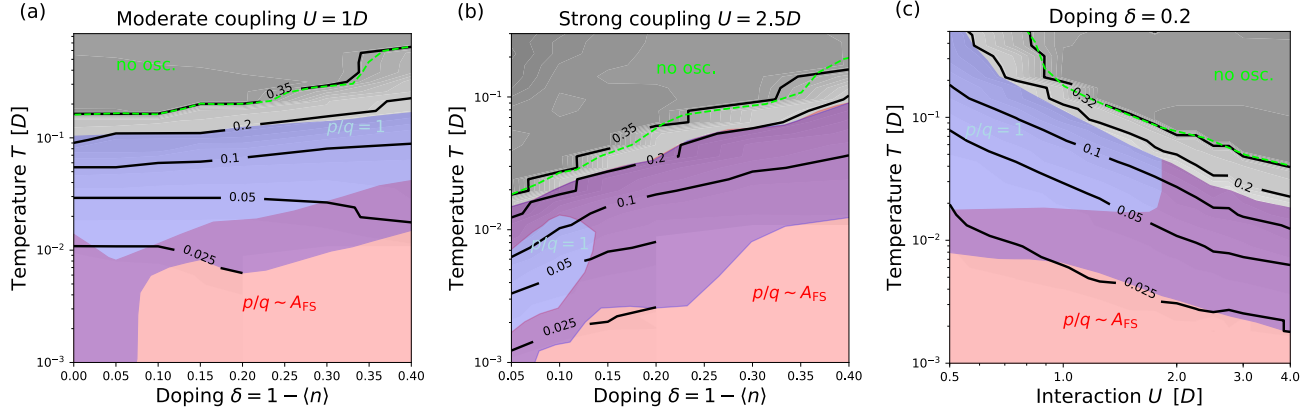


Figure 2. Phase diagrams with respect to the type of QOs observed: (a) and (b) the doping-temperature plane for $U = 1$ and $U = 2.5$; (c) interaction-temperature plane at $\delta = 0.2$. Red shading is purely SdH oscillations; purple is where both SdH and HF oscillations are observed; blue is where HF oscillations are dominant. Black shading and contours denote the value of the field where non-monotonic behavior starts in $1/\sigma_{dc}^{xx}(B)|_T$ (analogous to the white line in Fig. 1).

to control the chemical potential to maintain constant band filling in the self-consistent DMFT loop, which hinders its convergence.

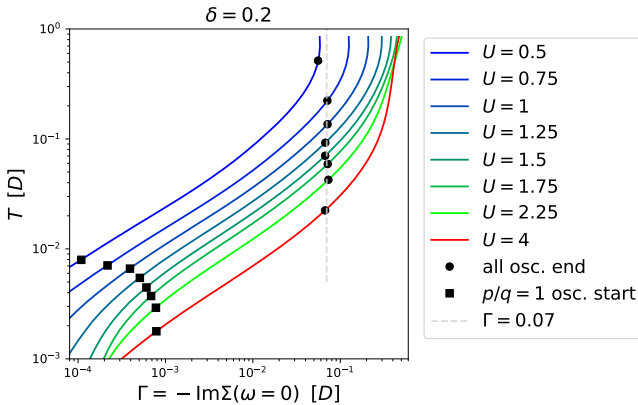


Figure 3. Relation between QOs and the scattering rate $\Gamma = -\text{Im}\Sigma(\omega = 0)$ and temperature T . Black squares indicate where $p/q = 1$ oscillations start with increasing T . Black circles indicate the temperature where all QOs cease; the circles fall on the line of fixed scattering rate $\Gamma \approx 0.07$. All data is for $\langle n \rangle = 0.8$ (i.e. $\delta = 0.2$), corresponding to Fig. 2(c).

Results. Fig. 1(a) shows the inverse conductivity at a moderate interaction strength $U = 1$ at band filling $\langle n \rangle = 0.8$ over a broad range of temperature and flux. At low temperatures, we clearly see prominent oscillations in the quantum limit (large p/q) where the system has wide gaps in ranges close to simple fractions, as well as the weaker QOs for lower fields corresponding to the Shubnikov-de Haas (SdH) regime. The onset of non-monotonic behavior is marked with the white line: it indicates the value of B where the first extremum in $1/\sigma_{dc}^{xx}$ is encountered, for a given T . As can be seen from the Fourier transform of the

oscillatory part of $1/\sigma_{dc}^{xx}(B^{-1})$ in Fig. 1(f), at low temperature (red spectrum) the oscillations have a frequency equal to roughly $p/q = \langle n \rangle/2$, which is consistent with the SdH oscillations in 2D. The frequency of SdH oscillations is given by the Onsager formula $F = \phi_0/(2\pi)^2 A_{FS}$, where A_{FS} is the cross-sectional area of the Fermi sea normal to the field direction; in 2D, $A_{FS} = (2\pi/a)^2 \langle n \rangle/2$ with a the lattice spacing, thus $F = \phi_0 a^2 \langle n \rangle/2$. The QOs have a very high harmonic content because the system is strictly 2D and ideally homogeneous. With increasing temperatures, the amplitude of these QOs is reduced in line with the Lifshitz-Kosevitch theory [2, 34].

Wholly unexpectedly, at elevated temperatures (purple and blue spectra in Fig. 1(g)), we see another type of QOs with a higher frequency; we will denote these as high-frequency (HF) oscillations. Converting the frequency to the fraction of the Brillouin zone area, we find that it corresponds to the total area of the BZ. This frequency is universal: it does not depend on any model parameter, in particular not on the electron density. These HF oscillations may coexist with the SdH oscillations (purple spectrum) or may be the dominant QOs (blue spectrum).

In Fig. 2 we show phase diagrams with respect to the type of oscillations observed in $1/\sigma_{dc}^{xx}(B)$, in the range of field $p/q \in [0.03, 0.15]$. With red we denote the regime where only SdH oscillations are observed; purple means both SdH and HF oscillations are present; blue is the regime where HF oscillations are dominant (the $p/q = 1$ peak is stronger than the $p/q \approx \langle n \rangle/2$ peak). The black shading and contours in the background denote the magnetic field for the onset of non-monotonic behavior (analogously to the white line in Fig. 1(a)). In the regime where visible oscillations are present only at $p/q > 0.15$, it is difficult to discern precisely the relative strength of two types of oscillations, and we cannot rule out the presence of weak SdH oscillations. Above the lime dashed line, no oscillations are observed.

tions are detectable at our level of accuracy, and there is at most a single maximum in the entire $1/\sigma_{dc}^{xx}(p/q < 1/2)$ curve.

The onset field for the significant oscillations (non-monotonic behavior) depends strongly on the coupling strength U and the doping $\delta = 1 - \langle n \rangle$; the oscillations are stronger in less correlated regimes (lower U and larger doping δ). The HF oscillations are pushed to higher temperatures with increasing doping; at a fixed doping, increasing the strength of interaction reduces the temperature needed to observe HF oscillations. The phase diagrams in Fig. 2 clearly document that the HF oscillations arise in *moderately correlated* regimes. To further corroborate this statement, in Fig. 3 we present a diagram that shows the effective scattering rate $\Gamma = -\text{Im}\Sigma(\omega = 0)$ at different temperatures for a range of interaction strengths U . The black squares denote the lower temperature where the HF oscillations become detectable; the black circles denote the temperature where all QOs cease. The results indicate that the HF oscillations appear for a sufficiently large scattering rate and a high enough temperature, i.e., it is a strong-interaction effect which emerges at intermediate temperatures. Large scattering Γ eventually kills all QOs, but the corresponding cut-off temperature strongly depends on U .

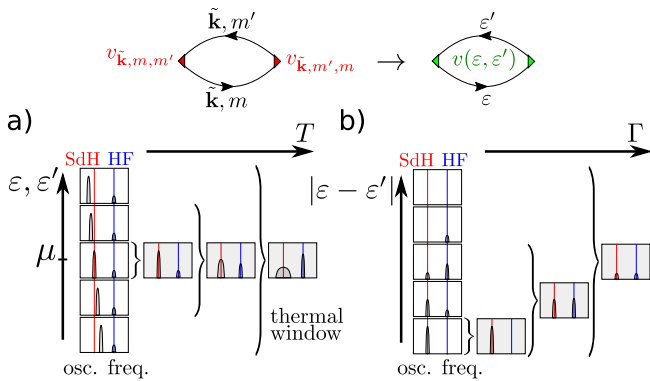


Figure 4. Illustration of the trends in oscillation spectra and the corresponding mechanisms. Top: diagrammatic representation of the Kubo bubble, at the level of DMFT. (\tilde{k}, m) denotes eigenstates of the non-interacting Hamiltonian (see [34] for details). The current (or velocity) vertices (red triangles) are rewritten in terms of two kinetic energies, and merged into a single vertex factor $v(\epsilon, \epsilon')$ (green triangles). Below: the oscillation spectra of $v(\epsilon, \epsilon')$. (a) trend with respect to temperature. At different $(\epsilon, \epsilon' \approx \epsilon)$ SdH oscillations are at different frequencies, while HF oscillations are always at the same frequency. (b) trend with respect to scattering rate. Values of v exhibit SdH oscillations at small $|\epsilon - \epsilon'|$, HF oscillations at intermediate $|\epsilon - \epsilon'|$, and no oscillations at large $|\epsilon - \epsilon'|$.

Discussion. The SdH oscillations are associated with the coherent part of the spectral function, i.e., with the quasiparticles. In correlated electron systems these can either be the Landau Fermi-liquid quasiparticles at the lowest temperatures or the resilient quasiparticles at intermediate

temperatures [35]; both correspond to the same frequency $p/q = \langle n \rangle/2$. The HF oscillations must have a different origin. We have verified that neither the Green's function nor the self-energy function Σ have an oscillatory component at the frequency of HF oscillations [34]. In particular, the transport scattering rate $\Gamma = -\text{Im}\Sigma(\omega = 0)$ was found to only oscillate with the SdH frequency.

The HF oscillations cannot be reproduced by a semi-classical theory since they are not associated with any specific trajectories of electrons in real space (and associated trajectories along the FS in the k space). Instead, the HF oscillations must be associated with the incoherent part of the spectral function away from the chemical potential which receives contributions from all parts of the BZ. At high temperature all electrons contribute to transport. The total area of the BZ is the only characteristic area in this regime, which appears to explain the universality of the frequency.

Beside the Green's function, the only remaining field-dependent factor contributing to the conductivity is the *electron velocity kernel*, which is a product of group velocities $\nabla_k \epsilon_k$ and may be expressed as a function of two kinetic-energy arguments, $v(\epsilon, \epsilon')$ (illustrated in the top part of Fig. 4). Depending on temperature, effective scattering rate and chemical potential, different (ϵ, ϵ') domains of v play a role. This comes as $\sigma_{dc}^{xx} \sim \int d\epsilon d\epsilon' v(\epsilon, \epsilon') f(\epsilon, \epsilon')$ [34] and $f(\epsilon, \epsilon')$ is a function that has a strong dependence on ϵ, ϵ' . In particular, only (ϵ, ϵ') such that $|\epsilon - \epsilon'| < \Gamma$ and $\epsilon^{(i)} - \mu < T$ give significant contributions. At low temperature, we observe that the SdH effect is already contained in $v(\epsilon, \epsilon')$, and that the peak in the oscillation spectrum of its relevant values moves with μ and coincides with $\langle n \rangle/2$. As the thermal window becomes bigger, more and more values of $v(\epsilon, \epsilon')$ enter the calculation, yet oscillate with different frequencies, depending on ϵ . This leads to dephasing and washing out of SdH oscillations. On the contrary, the HF oscillation is mild at any given ϵ , but is *always at the same frequency* ($p/q = 1$), thus its contribution accumulates with increasing T and can become the dominant effect. This is illustrated in Fig. 4(a). The domain of v that turns out to oscillate with the HF frequency is found at moderate $|\epsilon - \epsilon'|$. Therefore, as scattering rate Γ is increased, those values enter the calculation, and the HF oscillations become visible in σ_{dc}^{xx} . The values of $v(\epsilon, \epsilon')$ at large $|\epsilon - \epsilon'|$ do not oscillate with any particular frequency. As those get included at large Γ , all oscillations are ultimately overcome by the non-oscillatory contributions. This is illustrated in Fig. 4(b).

To our understanding, the interpretation of the HF oscillations in terms of any previously known QOs effects is not possible. For example, the magnetic interaction leads to combination frequencies, but the confusion between the SdH and HF components is possible only at half filling [1]. Magnetic breakdown (magnetic analog of Zener breakdown) can lead to QOs corresponding to the total BZ area,

but the topology of the FS in our problem is not such as to support this scenario [1].

Conclusion. We have uncovered a new aspect of magnetic quantum oscillations due to strong e-e interactions which emerges in the high-temperature regime where the ordinary SdH oscillations gradually die out. This regime has not been experimentally explored so far. It requires the combination of high temperatures and very high magnetic flux per unit cell. It is accessible in synthetic 2D systems with large lattice constant [41], such as cold atoms with artificial gauge fields [55–60] or twisted (moiré) materials [61]. Our results present a clear prediction for experiments, as the proposed oscillation frequency is universal, set solely by the lattice parameters, and thus easy to identify. Future work should address the role of non-locality of the self-energy and that of vertex corrections [28, 38, 62]. This will require the development of new sophisticated numerical approaches, capable of capturing short to intermediate-range non-local terms in very large magnetic cells, such as the diagrammatic Monte Carlo techniques formulated in real-frequency[63–67].

Computations were performed on the PARADOX supercomputing facility (Scientific Computing Laboratory, Center for the Study of Complex Systems, Institute of Physics Belgrade). J. V. acknowledges funding provided by the Institute of Physics Belgrade, through the grant by the Ministry of Education, Science, and Technological Development of the Republic of Serbia, as well as by the Science Fund of the Republic of Serbia, under the Key2SM project (PROMIS program, Grant No. 6066160). R. Ž. is supported by the Slovenian Research Agency (ARRS) under Program P1-0044 and Projects J1-1696 and J1-2458.

- [1] D. Schoenberg, *Magnetic oscillations in metals* (Cambridge Univ. Press, Cambridge, UK, 1984).
- [2] I. M. Lifshitz and A. M. Kosevich, Sov. Phys. JETP **2**, 636 (1956).
- [3] W. Kang, G. Montambaux, J. R. Cooper, D. Jérôme, P. Batail, and C. Lenoir, *Physical Review Letters* **62**, 2559 (1989).
- [4] J. Wosnitza, S. Wanka, J. Hagel, H. v. Löhneysen, J. S. Qualls, J. S. Brooks, E. Balthes, J. A. Schlueter, U. Geiser, J. Mohtasham, R. W. Winter, and G. L. Gard, *Physical Review Letters* **86**, 508 (2001).
- [5] M. V. Kartsovnik and V. G. Peschansky, *Low Temperature Physics* **31**, 185 (2005).
- [6] D. E. Soule, J. W. McClure, and L. B. Smith, *Physical Review* **134**, A453 (1964).
- [7] S. B. Hubbard, T. J. Kershaw, A. Usher, A. K. Savchenko, and A. Shytov, *Phys. Rev. B* **83**, 035122 (2011).
- [8] K. S. Novoselov, A. K. Geim, S. V. Morozov, D. Jiang, M. I. Katsnelson, I. V. Grigorieva, S. V. Dubonos, and A. A. Firsov, *Nature* **438**, 197 (2005).
- [9] Y. Zhang, Y.-W. Tan, H. L. Stormer, and P. Kim, *Nature* **438**, 201 (2005).

- [10] N. Doiron-Leyraud, C. Proust, D. LeBoeuf, J. Levallois, J.-B. Bonnemaison, R. Liang, D. A. Bonn, W. N. Hardy, and L. Taillefer, *Nature* **447**, 565 (2007).
- [11] S. E. Sebastian, N. Harrison, E. Palm, T. P. Murphy, C. H. Mielke, R. Liang, D. A. Bonn, W. N. Hardy, and G. G. Lonzarich, *Nature* **454**, 200 (2008).
- [12] S. E. Sebastian and C. Proust, *Annual Review of Condensed Matter Physics* **6**, 411 (2015).
- [13] A. D. Caviglia, S. Gariglio, C. Cancellieri, B. Sacépé, A. Fête, N. Reyren, M. Gabay, A. F. Morpurgo, and J.-M. Triscone, *Phys. Rev. Lett.* **105**, 236802 (2010).
- [14] P. Moetakef, D. G. Ouellette, J. R. Williams, S. J. Allen, L. Balents, D. Goldhaber-Gordon, and S. Stemmer, *Applied Physics Letters* **101**, 151604 (2012).
- [15] A. Carrington, *Reports on Progress in Physics* **74**, 124507 (2011).
- [16] Y. Cao, J. Y. Luo, V. Fatemi, S. Fang, J. D. Sanchez-Yamagishi, K. Watanabe, T. Taniguchi, E. Kaxiras, and P. Jarillo-Herrero, *Phys. Rev. Lett.* **117**, 116804 (2016).
- [17] F. Denef, S. A. Hartnoll, and S. Sachdev, *Phys. Rev. D* **80**, 126016 (2009).
- [18] S. A. Hartnoll and D. M. Hofman, *Phys. Rev. B* **81**, 155125 (2010).
- [19] D. V. Else, R. Thorngren, and T. Senthil, *Phys. Rev. X* **11**, 021005 (2021).
- [20] J. Knolle and N. R. Cooper, *Phys. Rev. Lett.* **115**, 146401 (2015).
- [21] A. Wasserman and M. Springford, *Advances in Physics* **45**, 471 (1996).
- [22] P. Schlottmann, *Phys. Rev. B* **77**, 195111 (2008).
- [23] A. Georges, G. Kotliar, W. Krauth, and M. J. Rozenberg, *Rev. Mod. Phys.* **68**, 13 (1996).
- [24] P. Limelette, P. Wzietek, S. Florens, A. Georges, T. A. Costi, C. Pasquier, D. Jérôme, C. Mézière, and P. Batail, *Phys. Rev. Lett.* **91**, 016401 (2003).
- [25] H. Terletska, J. Vučičević, D. Tanasković, and V. Dobrosavljević, *Phys. Rev. Lett.* **107**, 026401 (2011).
- [26] J. Vučičević, H. Terletska, D. Tanasković, and V. Dobrosavljević, *Phys. Rev. B* **88**, 075143 (2013).
- [27] J. Vučičević, D. Tanasković, M. J. Rozenberg, and V. Dobrosavljević, *Phys. Rev. Lett.* **114**, 246402 (2015).
- [28] J. Vučičević, J. Kokalj, R. Žitko, N. Wentzell, D. Tanasković, and J. Mravlje, *Phys. Rev. Lett.* **123**, 036601 (2019).
- [29] P. T. Brown, D. Mitra, E. Guardado-Sánchez, R. Nourafkan, A. Reymbaut, C.-D. Hébert, S. Bergeron, A.-M. S. Tremblay, J. Kokalj, D. A. Huse, P. Schauß, and W. S. Bakr, *Science* **363**, 379 (2018).
- [30] S. Acheche, L.-F. Arsenault, and A.-M. S. Tremblay, *Phys. Rev. B* **96**, 235135 (2017).
- [31] A. A. Markov, G. Rohringer, and A. N. Rubtsov, *Phys. Rev. B* **100**, 115102 (2019).
- [32] A. Khurana, *Phys. Rev. Lett.* **64**, 1990 (1990).
- [33] J. Merino and R. H. McKenzie, *Phys. Rev. B* **61**, 7996 (2000).
- [34] J. Vučičević and R. Žitko, “Conductivity in the Hubbard model: orbital effects of magnetic field,” (2021), *arXiv*.
- [35] X. Deng, J. Mravlje, R. Žitko, M. Ferrero, G. Kotliar, and A. Georges, *Phys. Rev. Lett.* **110**, 086401 (2013).
- [36] R. Žitko, D. Hansen, E. Perepelitsky, J. Mravlje, A. Georges, and B. S. Shastry, *Phys. Rev. B* **88**, 235132

(2013).

[37] E. Perepelitsky, A. Galatas, J. Mravlje, R. Žitko, E. Khatami, B. S. Shastry, and A. Georges, *Phys. Rev. B* **94**, 235115 (2016).

[38] A. Vranić, J. Vučičević, J. Kokalj, J. Skolimowski, R. Žitko, J. Mravlje, and D. Tanasković, *Phys. Rev. B* **102**, 115142 (2020).

[39] R. Peierls, *Zeitschrift fur Physik* **80**, 763 (1933).

[40] G. H. Wannier, *Rev. Mod. Phys.* **34**, 645 (1962).

[41] D. R. Hofstadter, *Physical Review B* **14**, 2239 (1976).

[42] L. Laloux, A. Georges, and W. Krauth, *Phys. Rev. B* **50**, 3092 (1994).

[43] J. Bauer and A. C. Hewson, *Phys. Rev. B* **76**, 035118 (2007).

[44] M. Potthoff and W. Nolting, *Phys. Rev. B* **59**, 2549 (1999).

[45] S. Okamoto and A. J. Millis, *Phys. Rev. B* **70**, 241104 (2004).

[46] R. W. Helmes, T. A. Costi, and A. Rosch, *Phys. Rev. Lett.* **101**, 066802 (2008).

[47] M. Snoek, I. Titvinidze, C. Tőke, K. Byczuk, and W. Hofstetter, *New Journal of Physics* **10**, 093008 (2008).

[48] R. Peters and N. Kawakami, *Phys. Rev. B* **89**, 155134 (2014).

[49] E. Brown, *Physical Review* **133**, A1038 (1964).

[50] K.-T. Chen and P. A. Lee, *Phys. Rev. B* **84**, 205137 (2011).

[51] M.-T. Tran, *Phys. Rev. B* **81**, 115119 (2010).

[52] D. Cocks, P. P. Orth, S. Rachel, M. Buchhold, K. Le Hur, and W. Hofstetter, *Phys. Rev. Lett.* **109**, 205303 (2012).

[53] P. Kumar, T. Mertz, and W. Hofstetter, *Phys. Rev. B* **94**, 115161 (2016).

[54] P. P. Orth, D. Cocks, S. Rachel, M. Buchhold, K. L. Hur, and W. Hofstetter, *Journal of Physics B: Atomic, Molecular and Optical Physics* **46**, 134004 (2013).

[55] D. Jaksch and P. Zoller, *New Journal of Physics* **5**, 56 (2003).

[56] F. Gerbier and J. Dalibard, *New Journal of Physics* **12**, 033007 (2010).

[57] J. Dalibard, F. Gerbier, G. Juzeliūnas, and P. Öhberg, *Reviews of Modern Physics* **83**, 1523 (2011).

[58] M. Aidelsburger, M. Atala, S. Nascimbène, S. Trotzky, Y.-A. Chen, and I. Bloch, *Phys. Rev. Lett.* **107**, 255301 (2011).

[59] M. Aidelsburger, M. Atala, M. Lohse, J. T. Barreiro, B. Paredes, and I. Bloch, *Phys. Rev. Lett.* **111**, 185301 (2013).

[60] H. Miyake, G. A. Siviloglou, C. J. Kennedy, W. C. Burton, and W. Ketterle, *Phys. Rev. Lett.* **111**, 185302 (2013).

[61] E. Y. Andrei, D. K. Efetov, P. Jarillo-Herrero, A. H. MacDonald, K. F. Mak, T. Senthil, E. Tutuc, A. Yazdani, and A. F. Young, *Nature Reviews Materials* **6**, 201 (2021).

[62] D. Bergeron, V. Hankevych, B. Kyung, and A.-M. S. Tremblay, *Phys. Rev. B* **84**, 085128 (2011).

[63] A. Taheridehkordi, S. H. Curnoe, and J. P. F. LeBlanc, *Phys. Rev. B* **99**, 035120 (2019).

[64] J. Vučičević and M. Ferrero, *Phys. Rev. B* **101**, 075113 (2020).

[65] A. Taheridehkordi, S. H. Curnoe, and J. P. F. LeBlanc, *Phys. Rev. B* **101**, 125109 (2020).

[66] A. Taheridehkordi, S. H. Curnoe, and J. P. F. LeBlanc, *Phys. Rev. B* **102**, 045115 (2020).

[67] J. Vučičević, P. Stipsić, and M. Ferrero, *Phys. Rev. Research* **3**, 023082 (2021).